Power dependence of terahertz carrier frequency in a plasma-based two-color generation process*

Zhao Ji(赵 骥)[a], Zhang Liang-Liang(张亮亮)[b], Luo Yi-Man(骆怡蔓)[b], Wu Tong(吴 同)[b], Zhang Cun-Lin(张存林)[b], and Zhao Yue-Jin(赵跃进)[a]†

[a] *Beijing Key Laboratory for Precision Optoelectronic Measurement Instrument and Technology, School of Optoelectronics, Beijing Institute of Technology, Beijing* 100081, *China*

[b] *Beijing Key Laboratory for Terahertz Spectroscopy and Imaging, Key Laboratory of Terahertz Optoelectronics, Ministry of Education, Capital Normal University, Beijing* 100048, *China*

(Received 13 May 2014; revised manuscript received 12 July 2014; published online 10 October 2014)

We conduct a frequency spectrum experiment to investigate terahertz (THz) emissions from laser-induced air plasma under different laser incident powers. The frequency spectra are measured using both air-biased-coherent detection and a Michelson interferometer. The red-shift of the THz pulse carrier frequency is observed as a response to increased pump power. These phenomena are related to plasma collisions and can be explained by the plasma collision model. Based on these findings, it is apparent that the tuning of the THz carrier frequency can be achieved through regulation of the pump beam.

Keywords: terahertz frequency, red-shift, plasma collision

PACS: 72.30.+q, 42.65.Tg **DOI:** 10.1088/1674-1056/23/12/127201

1. Introduction

Since it was first predicted in 1993, terahertz (THz) emission generated by a laser focused in the air has aroused a considerable amount of interest in various fields,[1,2] including material characterization, nondestructive evaluation, and biomedical and pharmaceutical testing.[3–7] An ultrashort laser fundamental (ω) and second harmonic (2ω) pulses are co-focused in the air to ionize the air molecules, and thus generate a THz wave through four-wave mixing.[8–12] In this model, a highly nonlinear and phase-sensitive asymmetric laser field can be generated, in which the bound gas-phase electrons can acquire a nonzero drift velocity and produce a free electron current with simultaneous emission of THz radiation in the far-field.[13] However, previous studies regarding THz generation performance in laser-induced air plasma have mainly concentrated on the intensity of the measured THz pulse, whereas carrier frequency information has been largely ignored.

In the present experiment, the intense THz radiation emitted from the ionized air plasma described above is observed to have a broader frequency band and higher power than that emitted from photoconductive antennae and electro-optic crystals. The frequency broadenings of the THz wave generated at various gas pressures[12] and in different gas environments[14] are measured. Then, we determine experimentally that the carrier frequency moves to the low frequency range if the pump power, $P_{\rm pump}$, of the laser is increased. This phenomenon can be observed using both the Michelson interferometer system and the air-biased-coherent-detection (ABCD) system. Finally, the redshift of the THz-pulse carrier frequency is discussed based on the plasma collision model.

2. Experimental methods and results

A schematic illustration of the THz ABCD setup is shown in Fig. 1. The THz field in this detection setup is detected through the measurement of the THz-field-induced second harmonic 2ω pulse.[15,16] The laser used is output from a Ti:sapphire regenerative amplifier (Spectra-Physics Hurricane), and has an 800-nm center wavelength, a 1-kHz repetition rate, and 50-fs pulse duration. The laser beam is split into two parts: a pump beam and a probe beam, and a 100-μm-thick type-I beta barium borate crystal is used in the pump beam to generate the second harmonic beam 2ω. A convex lens with a 150-mm effective focal length mixes the fundamental beam with the second harmonic 2ω beam at the air point in front of a parabolic mirror, PM1, which subsequently generates the THz wave. A half-wave plate and a Glan prism are placed in the pump beam path before the lens to allow $P_{\rm pump}$ to be adjusted. During operation, the superimposed fundamental and second harmonic optical fields tunnel-ionize the air and drive a time-dependent current, leading to THz emission in the forward direction. The THz emission is then collected and focused by two pairs of off-axis parabolic mirrors. The probe beam, focused by a 125-mm convex lens,

*Project supported by the National Natural Science Foundation of China (Grant Nos. 61377109 and 11374007) and the Support Program for Outstanding Ph. D. Advisors, China (Grant No. YB20101000701).

†Corresponding author. E-mail: yjzhao@bit.edu.cn

© 2014 Chinese Physical Society and IOP Publishing Ltd

co-propagates with the THz beam by passing through a hole on the back of the 4th parabolic mirror PM4 in the THz beam path. The THz and optical beams are then focused collinearly onto the same spot where the THz field induces the second-harmonic field, $E_{2\omega}^{\mathrm{THz}}$. A pair of wire-shaped electrodes with a 1-mm gap is placed across the beam focus point, with a $\sim$ 2 kV, 500-Hz ac bias (synchronized with the laser repetition rate), which induces the second-harmonic field, $E_{2\omega}^{\mathrm{LO}}$. The sum of the two fields ($E_{2\omega}^{\mathrm{THz}} + E_{2\omega}^{\mathrm{LO}}$), is filtered by a pair of 400-nm band pass filters and collected in the photomultiplier tube (PMT). The signal from the PMT is measured using a lock-in amplifier following the 500-Hz bias modulation frequency. The area within a black rectangular frame in Fig. 1 is purged by the nitrogen gas to eliminate water absorption lines and the relative humidity in the chamber is below 4%.

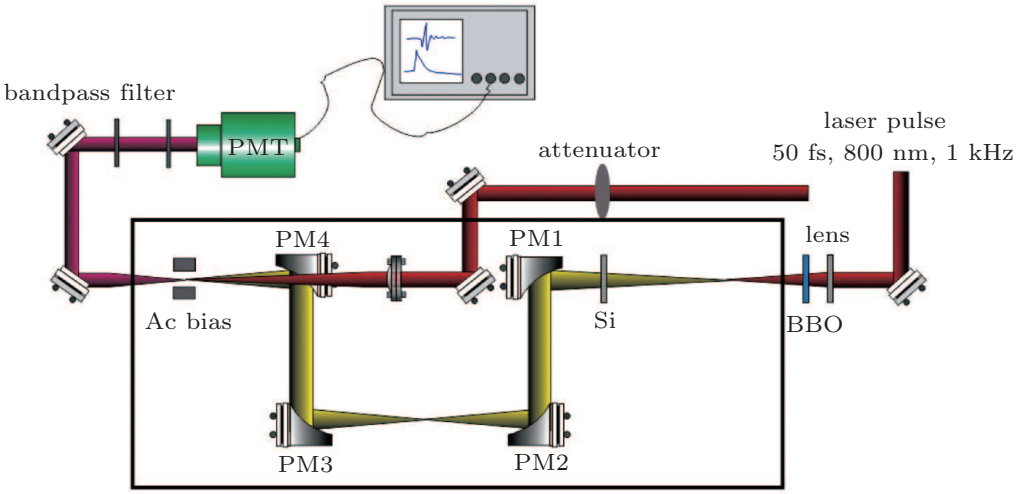


Fig. 1. (color online) Schematic diagram of the ABCD experimental system.

Figure 2 shows the THz frequency spectra for different P_{pump} values in the ABCD system. Here, the pump intensity is increased while the probe power is kept constant and the spectrum of the generated THz radiation is obtained by the Fourier transform of the time-domain signal. We can see from the frequency spectrum that the carrier frequency decreases from 15.30 THz to 12.26 THz. The inset shows the Fourier components of the wave forms.

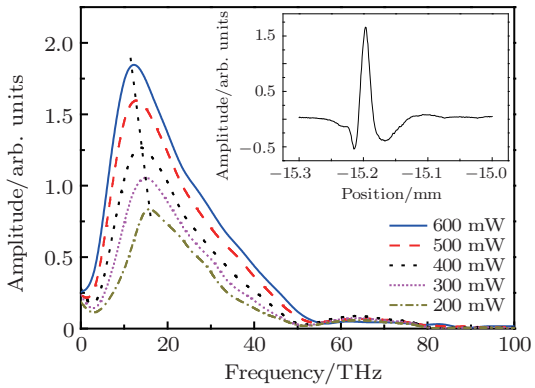


Fig. 2. (color online) Frequency spectra for the different pump powers, measured using the ABCD system. The dashed line indicates the shift in the central frequency and the inset gives the detected THz time-domain waveform of the 600-mW pump power.

As a result of the particular THz detection method used in the ABCD system, the THz frequency-domain spectrum is easily affected by the change in the pulse-width of the probe beam. In order to further verify our experimental results, we use the Michelson interferometer system instead, which can detect the THz signal directly. Figure 3 shows a schematic of the Michelson interferometer setup. Here, THz radiation is generated by mixing the fundamental frequency with its second harmonic, which is identical to the production method of the ABCD system. A 0.4-mm-thick, high-resistivity silicon wafer is used as a THz beam splitter and the THz radiation is detected by a Golay cell equipped with a 6-mm-diameter diamond input window (Microtech SN:220712-D). It has an approximately flat response over a broad spectral range. The voltage signal of the detector is fed into a lock-in amplifier following 15-Hz modulation frequency. The system is purged with dry nitrogen gas to eliminate the absorption of the water vapor in the ambient air and, during operation, the relative humidity is below 4%. The corresponding THz frequency spectrum can then be obtained using the Fourier transform of the autocorrelation trace.

Figure 4 gives the frequency–domain spectra of the THz emission, and the redshift of the carrier frequency can be observed. Compared to the PMT, which functions as the second harmonic detector in the ABCD system, the Golay cell can directly detect the THz signal (which can be easily influenced by the surrounding environmental factors), rendering the THz

spectrum curve smoother than that generated using the PMT. As the high resistivity of silicon affects the THz absorption, an absorption peak can be observed in the THz frequency spectrum generated by the Michelson interferometer system. It is apparent that the carrier frequency decreases as P_{pump} changes from 200 mW to 600 mW. The inset of Fig. 4 shows a time-domain spectrum of the Michelson interferometer system.

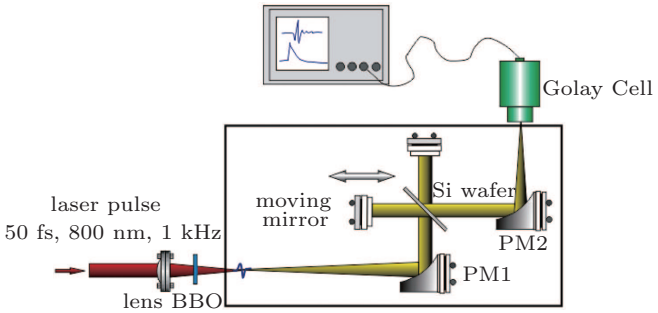


Fig. 3. (color online) Schematic diagram of the Michelson interferometer system PM1, PM2: Parabolic mirrors.

Figure 5 shows the linear variations of carrier frequency with P_{pump} in the Michelson system (a) and the ABCD system (b) and their slopes are found to be $k_{\text{ABCD}} = 0.387k_{\text{Michelson}} = 0.379$ and $k_{\text{ABCD}} = 0.387$, respectively. In the two different sets of detection systems, the carrier frequencies decrease linearly with P_{pump} increasing in similar slopes.

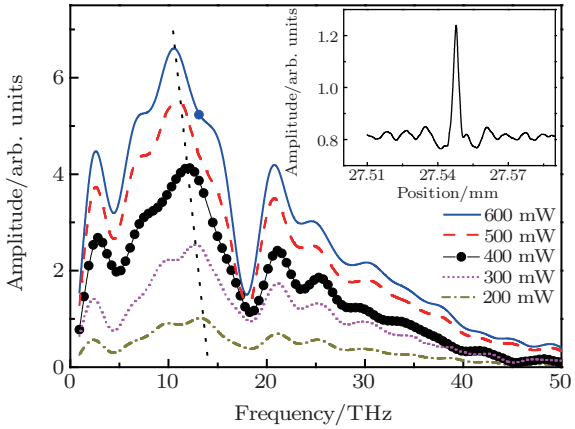


Fig. 4. (color online) Frequency spectra for the different pump powers, measured using the Michelson interferometer system. The dashed line indicates the shift of the central frequency. The inset gives the detected autocorrelated trace of the THz signal for a 600-mW pump power.

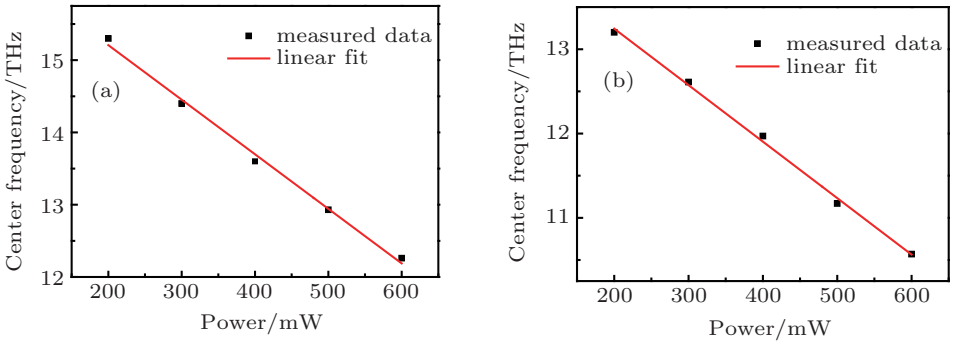


Fig. 5. (color online) (a) Linear fit of the central frequency versus pump power measured in the ABCD system. The slope of the curve is $k = 0.387$. (b) The linear fit of the central frequency versus the pump power, measured in the Michelson interferometer system. The slope of the curve is $k = 0.379$.

3. Discussion

The reason for the change in carrier frequency in response to different P_{pump} values relates to the THz generation process, which can be understood on a phenomenological basis of involving a four-wave mixing process in plasma. THz waves are generated from laser-induced air plasma. Therefore, electrons, ions, and neutral particles that exist in the plasma collide with each other, and the interactions among these particles can cause interference in the plasma state.[17] As a result of these collisions within the plasma, it can be deduced that the redshift of the THz carrier frequency may be affected by the number of ions per unit volume, N_0, which is determined by P_{pump}.[18] This can be expressed as

$$\delta_\nu = \frac{1}{2\pi} N_0 v \sigma, \tag{1}$$

where δ_ν is the change in carrier frequency, v is the relative speed of the atom, and σ is the collision cross section. The carrier frequency moves to the low frequency region with the increase of P_{pump}, and the carrier frequency is proportional to the number of plasma ions per unit volume, i.e. $\delta_\nu \propto N_0$. With the increase of laser power, N_0 increases proportionally, i.e. $\delta_\nu \propto P_{\text{pump}}$. As indicated in Fig. 5, the THz carrier frequency is related to P_{pump}, and it can be controlled by the laser power. This inference is supported by our experimental results. Such a behavior reveals that the THz carrier frequency may be related to the number of ions and can be controlled by changing the pump power.

4. Conclusion

The results presented in this paper demonstrate that redshift of the carrier frequency of THz pulses generated from

laser-induced air plasma occurs with the enhancement of P_{pump}. Through analysis of the carrier frequency response to varying P_{pump}, using both the ABCD detection system and a Michelson interferometer, it is apparent that the carrier frequency moves to the low frequency range by increasing the laser pump power. This phenomenon can be explained by using the plasma collision model and adopting the number of ions per unit volume as a parameter as well.

Acknowledgment

We are grateful to Cheng Gong for his useful discussion.

References

[1] Hamster H, Sullivan A, Gordon S, White W and Falcone R W 1993 *Phys. Rev. Lett.* **71** 2725
[2] Hamster H, Sullivan A, Gordon S and Falcone R W 1994 *Phys. Rev. E* **49** 671
[3] Ferguson, Bradley and Zhang X C 2002 *Nat. Mater.* **1** 26
[4] Li Y T, Wang W M, Li C and Sheng ZM 2012 *Chin. Phys. B* **21** 095203
[5] Pickwell E and Wallace V P 2006 *J. Phys. D: Appl. Phys.* **39** R301
[6] Kim and Seongsin M 2006 *Appl. Phys. Lett.* **88** 153903
[7] Wu S Q, Liu J S, Wang S L and Hu B 2013 *Chin. Phys. B* **22** 104207
[8] Hua Z, Karpowicz N and Zhang X C 2006 *Appl. Phys. Lett.* **88** 261103
[9] Kress M, Löffler T, Eden S, Thomson M and Roskos H G 2004 *Opt. Lett.* **29** 1120
[10] Kim K Y, Glownia J H, Taylor A J and Rodriguez G 2007 *Opt. Express* **15** 4577
[11] Bartel T, Gaal P, Reimann K, Woerner M and Elsaesser T 2005 *Opt. Lett.* **30** 2805
[12] Xu X, Dai J M and Zhang X C 2006 *Phys. Rev. Lett.* **96** 075005
[13] Karpowicz N, Lu X F and Zhang X C 2009 *Laser Phys.* **19** 1535
[14] Lu X F, Karpowicz N and Zhang X C 2009 *J. Opt. Soc. Am. B* **26** A66
[15] Dai J M, Xu X and Zhang X C 2006 *Phys. Rev. Lett.* **97** 103903
[16] Karpowicz N, Dai J M, Lu X F, Chen Y Q, Yamaguchi M, Zhao H W, Zhang X C, Zhang L L, Zhang C L, Price-Gallagher M, Fletcher C, Mamer O, Lesimple A, Johnson and Keith 2008 *Appl. Phys. Lett.* **92** 011131
[17] Lu T X and Lu Y Q 2009 *The Principle and Application of Laser Spectroscopy*, 2nd edn. (Hefei: University of Science and Technology of China Press) pp. 134, 135
[18] Karpowicz N, Lu X F and Zhang X C 2009 *J. Mod. Opt.* **56** 1137